Research Square

Preprints are preliminary reports that have not undergone peer review.
They should not be considered conclusive, used to inform clinical practice,
or referenced by the media as validated information.

Baseline Distribution and Ecological Risks of Silver in Multi-Environmental Media of the Northeastern Tibetan Plateau: Implications for Weather Modification

Han Huibang
Chinese Academy of Sciences
Zhang Yuxin
nuistzyx@126.com
Qinghai Weather Modification Center
Zhang Liyan
Qinghai Weather Modification Center
Guo Shiyu
Qinghai Weather Modification Center
Hou Yonghui
Qinghai Weather Modification Center
An Lin
Qinghai Weather Modification Center
Zhang boyue
Qinghai Weather Modification Center

Research Article

Keywords:

Posted Date: November 10th, 2026

DOI: https://doi.org/10.21203/rs.3.rs-11371334/v1

License: This work is licensed under a Creative Commons Attribution 4.0 International License.
Read Full License

Additional Declarations: No competing interests reported.

Baseline Distribution and Ecological Risks of Silver in Multi-Environmental Media of the Northeastern Tibetan Plateau: Implications for Weather Modification

Han Huibang [a,b,c,d], Zhang Yuxin[c,d*], Zhang Liyan[c,d], Guo Shiyu[c,d], Hou Yonghui[c,d], An Lin[c,d], Zhang boyue[c,d]

[a]*Northwest Institute of Eco-Environment and Resources, Chinese Academy of Sciences, Lanzhou, 730000, China*

[b]*University of Chinese Academy of Sciences, Beijing, 100049, China*

[c]*Qinghai Weather Modification Center, Xining 810000, China*

[d]*Key Laboratory for Disaster Prevention and Mitigation in Qinghai Province, Xining 810000, China*

Corresponding author:Zhang Yuxin Email:nuistzyx@126.com

ABSTRACT

Silver ions (Ag^+) are increasingly recognized as emerging technological contaminants driven by green energy expansion, as well as exclusive environmental tracers for artificial weather modification operations. However, their multi-sphere environmental baseline in sensitive alpine ecosystems remains largely unknown. This study constructs the first comprehensive multi-medium Ag^+ dataset (116 soil, 77 surface water, and 58 precipitation samples collected from 2023 to 2024) across Qinghai Province on the northeastern Tibetan Plateau to systematically decode its occurrence, migration mechanisms, and associated risks. Results indicate that while the regional multi-sphere environment maintains a high degree of baseline purity—with aqueous concentrations remaining two orders of magnitude below WHO thresholds—pedological evaluation indices reveal a shifting baseline toward a "slightly polluted" state. A distinct spatial decoupling was identified: terrestrial accumulation hotspots concentrate in the industrialized eastern catchments, directly reflecting ground-based manufacturing emissions, whereas atmospheric deposition peaks in the western arid regions. This atmospheric anomaly uniquely traces the precipitation "scavenging effect" of silver iodide (AgI) cloud-seeding catalysts. Regarding environmental risks, the inherently high biological toxicity of silver amplifies localized ecological stress, resulting in approximately 1%

of eastern soils exhibiting moderate ecological risk. Crucially, while chronic non-carcinogenic health risks from soil and surface water exposure are universally negligible (HQ < 1) across all demographics, episodic health hazards emerged exclusively through the direct ingestion of untreated precipitation in active cloud-seeding zones. These findings provide vital scientific benchmarks and management implications for balancing modern industrial development and regional cloud-water resource exploitation while safeguarding the "Asian Water Tower."

Keywords: Silver ions; Emerging technological contaminant; Artificial weather modification; Scavenging effect; Ecological risk assessment; Tibetan Plateau.

1.Introduction

Heavy metal contamination represents a persistent threat to global ecological integrity due to the non-degradable nature and high bioaccumulation potential of these elements (Li et al., 2018; Oves et al., 2012; Rachwał et al., 2017; Wu et al., 2018). While traditional industrial emissions and agricultural intensification have historically driven the accumulation of metals in terrestrial and aquatic ecosystems (Ahamed et al., 2010; Guan et al., 2024; Kumar et al., 2021; Li et al., 2024; Liu et al., 2024), the global transition toward green energy and the rapid expansion of high-technology industries have introduced contaminants of emerging concern. Among these metallic pollutants, silver (Ag) requires particular attention as a critical emerging technological contaminant. Beyond traditional applications, the modern consumption of silver has expanded exponentially due to the widespread use of this metal in advanced electronics and, importantly, the massive utilization of it as a key component in photovoltaic cells (Newman et al., 2024; Schluesener and Schluesener, 2013; Zhao et al., 2010). This extensive industrial throughput inevitably accelerates the risks of environmental release through localized mining, intensive manufacturing emissions, and waste disposal (Yang et al., 2023). For regions undergoing the large-scale deployment of solar infrastructure, such as Qinghai Province, China, which serves as a crucial national base for the production of green energy (Qu et al., 2025; Wang et al., 2024), the intensive installation of photovoltaic arrays presents unique and unprecedented challenges regarding the localized exploitation of

silver and the potential pathways for environmental contamination.

Although metallic silver is relatively inert, the environmental toxicity, potential for bio-concentration, and ecological hazards of this metal are strongly dependent on chemical speciation (Ratte, 1999; Rezvani et al., 2019). Free silver ions (Ag^{+}) constitute the most chemically reactive, bioavailable, and toxic form of this element, capable of disrupting the structure of microbial communities and the health of aquatic organisms even at trace levels (Choi et al., 2008; Rezvani et al., 2019). Crucially, aside from the footprint of industrial manufacturing, silver ions function as an exclusive environmental tracer for the technologies of artificial weather modification (Fisher et al., 2018; Hua et al., 2025). In alpine and arid regions with ecological vulnerability, silver iodide (AgI) is widely introduced into the upper troposphere as a highly efficient cloud-seeding catalyst to stimulate the formation of rain and snow (Bruintjes, 1999; Chen and Xiao, 2010). Once released into atmospheric clouds, AgI particles undergo a complex pathway of multi-sphere migration governed by the ``precipitation scavenging effect''. Atmospheric silver is effectively intercepted and washed out by falling raindrops, directly entering the vectors of transient precipitation. Subsequently, through precipitation deposition and surface runoff, this ionic silver infiltrates the regional hydrosphere and ultimately accumulates in the solid-phase matrix of the soil (Panyala et al., 2008). Consequently, tracking the environmental behavior of Ag^{+} provides a unique dual perspective to analyze both the stress of modern high-technology industries and intentional meteorological interventions at the regional scale.

The Tibetan Plateau, universally recognized as the Third Pole'' and the Asian Water Tower'', functions as a vital barrier of ecological security that sustains downstream ecosystems and the major river systems of Asia (Chen et al., 2015; Yao et al., 2012). Qinghai Province, situated on the northeastern margin of the plateau, encompasses highly sensitive ecological corridors, including the Qilian Mountains and the ``Three Rivers Source'' region---the source of the Yellow, Yangtze, and Lancang rivers (Han et al., 2023; Ma et al., 2021). Because of the critical importance of these areas in the ecological replenishment of regional water, these alpine catchments serve as core strategic zones for long-term and intensive operations of artificial precipitation enhancement (Luo Han, 2023; Wang et al., 2024). Despite these emerging threats, the understanding of heavy metal contamination on

the plateau remains uneven. Current assessments of environmental quality on the plateau remain heavily biased toward conventional heavy metals, such as arsenic (As), cadmium (Cd), lead (Pb), and chromium (Cr) (Chang et al., 2017; He and Gao, 2016; Hu et al., 2022; Sai et al., 2022; Yawei et al., 2017; Zhou et al., 2020). By contrast, baseline data regarding the environmental distribution, multi-sphere partitioning, and spatial heterogeneity of silver remain extremely scarce on the plateau. The existing knowledge relies predominantly on simulations in the laboratory or datasets of urban sewage sludge rather than on in-situ monitoring across multiple media in alpine environments. This critical gap in data severely hinders the accurate characterization of the risks to ecosystems and human health posed by this emerging contaminant in sensitive alpine regions.

To address this deficiency in data, this study aims to determine the concentration and the spatial distribution of silver ions in the northeastern region of the Tibetan Plateau. Through the comprehensive sampling of multiple media, including soil, surface water, and precipitation across Qinghai Province, this research systematically assesses the levels of contamination and the associated risks to the ecosystem. The findings of this study will establish a critical baseline for understanding the fate of silver in the environment of alpine ecosystems, and will provide valuable data to the global inventory of contaminants of emerging concern.

2.Materials and methods

2.1. Research region

The Tibetan Plateau, located in northwest China, covers an area of approximately 265×10^4 km^2, accounting for one-quarter of the total landmass of the nation. Covering the entire regions of Qinghai and Tibet, this area is the highest and largest plateau globally, with an average altitude exceeding 4,000 m. Often referred to as the Roof of the World" and the Third Pole of the Earth", the plateau functions as the ``Asian Water Tower". This region serves as the headwaters for ten major river systems in Asia, including the Yangtze, Yellow, Brahmaputra, Ganges, and Indus rivers, which collectively sustain approximately 40% of the global population (Xu et al., 2019; Zhao et al., 2024). Qinghai Province, situated in the northeastern sector of the Tibetan Plateau, spans approximately 1,200 km from east to west

and 800 km from north to south, encompassing a total area of roughly 72×10^4 km^2. The region exhibits a distinct gradient of elevation, generally rising from the northeast and northwest towards the southwest, with an average elevation exceeding 3,000 m above sea level. The province is geographically defined by major mountain ranges to the northeast, including the Qilian Mountains, the Qinghai South Mountains, and the Tuole South Mountains. The northwestern sector is dominated by the arid Qaidam Basin, while the southern region contains the ``Three Rivers Source" area---the source of the Yellow, Yangtze, and Lancang rivers. Geomorphologically, Qinghai represents a unique zone of transition where three distinct topographic units converge: the Tibetan Plateau, the Inland Arid Basin, and the Loess Plateau(Fig. 1). Climatically, the province is governed by a typical continental climate, which significantly influences the geochemical migration of elements on the surface (Tang et al., 2023; Zhang et al., 2023; Zhang et al., 2021). In recent years, Qinghai has become a central hub for intensive anthropogenic interventions, specifically the large-scale deployment of infrastructure for photovoltaic green energy in the Qaidam Basin and extensive operations of artificial weather modification (cloud seeding) across the Qilian Mountains and the Sanjiangyuan region. These localized activities make this province an ideal natural laboratory for tracing the migration of technological contaminants of emerging concern, such as silver ions, across multiple spheres.

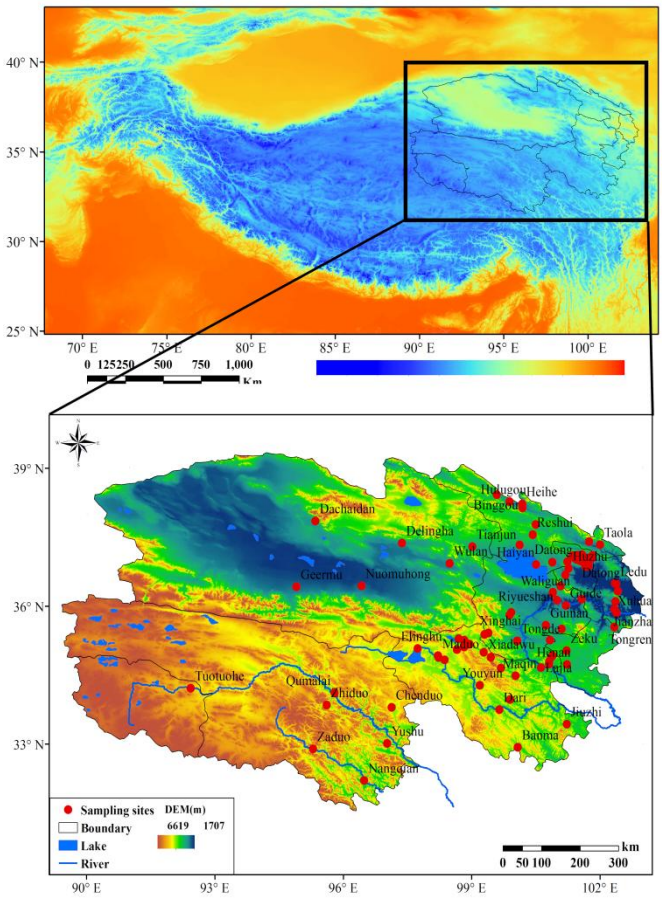


Fig.1. Digital elevation model (DEM) image map of the research region and the sampling locations

2.2 Sample and data collection

To ensure spatial representativeness across the heterogeneous terrain of Qinghai Province, a systematic campaign for sampling was conducted from 2023 to 2024. A total of 251 environmental samples were collected from coordinates identified by GPS, comprising 116 samples of soil, 77 samples of surface water, and 58 samples of precipitation(Fig. 1). During the sampling and pre-treatment of soil, field operations strictly adhered to the Guidance on Soil Sampling Techniques (GB/T 36197-2018). To minimize heterogeneity within sites, a diagonal strategy for five-point composite sampling was employed at each location. Crude samples were homogenized and reduced using the method of coning and quartering to retain a representative sub-sample (< 1kg). Debris, including the roots of plants and gravel, was manually removed, and the samples were sealed in labeled bags of low-density polyethylene (LDPE) to prevent cross-contamination during transport. In the

laboratory, the samples of soil underwent air-drying in a controlled environment at 35±5°C. To prevent contamination by metals, the dried aggregates were disaggregated using a wooden mallet and passed through a nylon sieve of 2 mm. The undersize fraction was further ground using an agate ball mill and sieved through a nylon mesh of 1 mm prior to digestion.

The collection of surface water followed the Standard Test Methods for Drinking Water (GB/T 5750.2-2023). Aliquots of 200 to 500 mL were collected in acid-washed bottles of LDPE. To preclude secondary pollution caused by human contact, operators utilized clean protective gloves of polypropylene throughout the procedure. To prevent the precipitation or the adsorption of silver ions (Ag^+) onto the walls of the containers, all aqueous samples were immediately filtered in-situ through a cellulose acetate membrane of 0.45um and acidified to a pH <2 using ultrapure concentrated HNO_3.

All processed samples were transported to the Centre Testing International Group (CTI) for geochemical analysis. The concentration of silver ions (Ag^+) was quantified using Inductively Coupled Plasma Mass Spectrometry (ICP-MS, Agilent 7900, USA), which was selected for the high sensitivity and wide dynamic range of this instrument. Stringent protocols for quality assurance and quality control (QA/QC) were implemented, including the use of procedural blanks, duplicate samples, and certified reference materials (CRMs) to ensure analytical precision and accuracy, with recoveries ranging between 95% and 105%.

2.3 Evaluation methodology

The accurate quantification of risks from heavy metals is imperative to mitigate the impacts of rapid regional development on the environment (Li et al., 2018; Ramachandra et al., 2018). To systematically evaluate the status of contamination and the threats to the ecology posed by silver in this alpine ecosystem, this research applies a suite of established geochemical indices. Specifically, the Single Factor Pollution Index (P_{Ag}), the Nemerow Pollution Index (($P_{N\text{-}Ag}$)), the Geo-accumulation Index (I_{geo}), and the Potential Ecological Risk Index (ERI) were calculated to provide a multi-dimensional assessment of the quality of soil and sediment (Liu et al., 2018). To address the distinct physicochemical behaviors of silver in matrices of solid and aqueous phases, the models for evaluation were strictly categorized to prevent the misapplication of methodology(Table 2).

2.3.1 Soil Pollution and Ecological Risk Assessment

For the pedological environment, accumulation and ecological risks were quantified utilizing the Single Factor Pollution Index (P_{Ag}), Nemerow Pollution Index ($P_{N\text{-}Ag}$), Geo-accumulation Index (I_{geo}), and the Potential Ecological Risk Index (ERI). The P_{Ag} and $P_{N\text{-}Ag}$ were calculated to assess direct contamination levels, while I_{geo} was employed to discriminate anthropogenic enrichment from natural lithogenic fluctuations (Hakanson, 1980; Muller, 1969):

$$P_{\mathrm{Ag}} = \frac{C_{Ag}}{S_{Ag}}$$

$$P_{\mathrm{N\text{-}Ag}} = \frac{\sqrt{P_{\mathrm{avg}}{}^{2} + P_{\mathrm{max}}{}^{2}}}{2}$$

$$I_{\mathrm{geo}} = \log_2\left(\frac{C_{\mathrm{Ag}}}{1.5 S_{Ag}}\right)$$

Here, C_{Ag} represents the measured concentration in the soil, and S_{Ag} represents the geochemical background value. The selection of appropriate values for S_{Ag} is critical for the accurate characterization of risk. Due to the scarcity of specific data for the geochemical baseline of silver in the unique alpine terrain of the Tibetan Plateau, the background concentration of silver in the soils of China (100 ug kg^{-1}) was adopted as a representative proxy for the lithogenic background. To rigorously evaluate the potential risks to both the integrity of the ecosystem and the health of humans, the thresholds of reference were aligned with stringent regulatory standards. The evaluation incorporates the Standards for Drinking Water Quality (GB 5749-2022) and the Standard for Groundwater Quality (GB/T 14848-2017), which correspond with the maximum allowable concentration (MAC) of silver of 50 ug L^{-1} established by the World Health Organization (Edition, 2011).

To quantify the biological threat posed by contamination by silver, the Potential Ecological Risk Index (ERI) was calculated. The core advantage of this approach, originally proposed by (Hakanson, 1980), lies in the ability of the index to reflect the sensitivity of biological communities to specific toxic substances, thereby showing the potential harm to the ecosystem (Suresh et al., 2012). For a specific contaminant, the factor of potential ecological risk (ERI) is calculated as follows:

$$ERI = T_{Ag} \times P_{Ag} = T_{Ag} \times \frac{C_{Ag}}{S_{Ag}}$$

Here, T_{Ag} represents the factor of toxic response. Reflecting the high toxicity of silver to organisms in terrestrial and benthic environments, T_{Ag} was assigned a conservative value of 19 (Lin, 2009). The thresholds of classification for P_{Ag}, $P_{N\text{-}Ag}$, I_{geo}, and ERI remain consistent with standard frameworks of geochemistry.

2.3.2. Assessment of the quality of water and precipitation

Given that the I_{geo} and ERI models are designed exclusively for the partitioning of solid phases and the geology of the background, the application of these models to transient aqueous phases is invalid. Consequently, the environmental quality of surface water and precipitation was evaluated directly by benchmarking the measured concentrations of Ag^{+} against stringent regulatory thresholds. The limits of reference incorporate the Standards for Drinking Water Quality (GB 5749-2022) and the Standard for Groundwater Quality (GB/T 14848-2017), which correspond with the maximum allowable concentration (MAC) of silver of 50 ug L^{-1} established by the World Health Organization (Edition, 2011).

2.3.3. Assessment of risks to the health of humans

A comprehensive assessment of risks to the health of humans (HHRA) was conducted to estimate the non-carcinogenic risks for adults and children, applying models endorsed by the United States Environmental Protection Agency (USEPA). Heavy metals in matrices of the environment pose risks primarily through distinct routes of exposure. For the pedological environment (soil), exposure was evaluated across three pathways: incidental ingestion, dermal contact, and the inhalation of particulates. For aqueous matrices (surface water and precipitation), direct ingestion was identified as the predominant vector of exposure. The Hazard Quotient (HQ) for specific pathways is calculated as follows:

$$HQ = \sum \left(\frac{ADI_i}{RFD_i} \right)$$

Here, ADI_i represents the Average Daily Intake (mg $kg^{-1}d^{-1}$) derived from standardized parameters of exposure from the USEPA. The Average Daily Intake for each specific pathway was calculated using the following deterministic equations(Table 1):

236 $$ADI_{\text{ingestion}} = \frac{C_{Ag} \times IR_1 \times CF \times EF \times ED}{BW \times AT}$$

237 $$ADI_{\text{drinking}} = \frac{C_{Ag} \times IR_3 \times ABS_1 \times EF \times ED}{BW \times AT}$$

238 $$ADI_{\text{contact}} = \frac{C_{Ag} \times CF \times SA \times AF \times ABS_2 \times EF \times ED}{BW \times AT}$$

239 $$ADI_{\text{inhalation}} = \frac{C_{Ag} \times IR_2 \times EF \times ED}{BW \times PET \times AT}$$

240 **Table1**

241 Parameters of silver ions exposure levels and their reference values

number	parameters	implication	unit	adult	child
1	IR_1	Daily intake rate	mg d^{-1}	100	200
2	IR_2	Soil uptake rate	mg d^{-1}	14.5	7.5
3	IR_3	Water intake rate	L d^{-1}	2	0.64
4	ED	Duration of exposure	a	24	6
5	BW	Average weight	kg	56.8	15.9
6	SA	Exposed skin area	cm^2	5057	2448
7	AF	Skin adhesion coefficient	mg·cm^{-1}·d^{-1}	0.07	0.2
8	AT	Average exposure time	d	8760	2190
9	PEF	Particulate matter release factor	mg^3 kg^{-1}	1.36×10^9	
10	ABS_1	Gastrointestinal absorption factor	/	0.57	
11	ABS_2	Skin absorption factor	/	0.001	
12	CF	Transformation factor	mg kg^{-1}	10^{-6}	
13	C_{Ag}	Measured value	mg kg^{-1}/ug L^{-1}		
14	EF	Frequency of soil exposure	d a^{-1}	350	

242 Furthermore, RFD_i represents the reference dose. Due to the absence of established
243 chronic values of RfD specifically for silver across all pathways in standard databases of
244 toxicology, this study cautiously adopted the toxicological parameters of cadmium (Cd) as a

conservative proxy for silver, given the similar behaviors in geochemistry and high characteristics of bioavailability of these metals in matrices of the environment. This approach aligns with the precautionary principle in the assessment of environmental risks. This research adopts the reference doses of cadmium for the pathways of ingestion, dermal contact, and inhalation as $3.0\times10^{-3}mg^3\ kg^{-1}d^{-1}$, $6\times10^{-5}mg^3\ kg^{-1}d^{-1}$ and $2.86\times10^{-7}mg^3\ kg^{-1}d^{-1}$ (Long et al., 2024).

Table 2

Classification and description of P_{Ag}, $P_{N\text{-}Ag}$, I_{geo}, ERI, and HQ

P_{Ag}		$P_{N\text{-}Ag}$		I_{geo}		ERI		HQ	
Value	Assessment level	Value	Assessment level	Value	Assessment level	Value	Enrichment Level	Value	Enrichment Level
$P_{Ag}\leq1$	Unpolluted	$P_{N\text{-}Ag}\leq0.7$	Clean/Safe	$I_{geo}\leq0$	Practically uncontaminated	ERI＜40	Low risk	HQ＜1	Negligible
$1<P_{Ag}\leq2$	Mildly pollution	$0.7<P_{N\text{-}Ag}\leq1$	Still clean/warning limit	$0<I_{geo}\leq1$	Uncontaminated to moderately contaminated	40≤ERI＜80	Moderate risk	HQ≥1	Exist
$2<P_{Ag}\leq3$	Slightly polluted	$1<P_{N\text{-}Ag}\leq2$	Slightly polluted	$1<I_{geo}\leq2$	Moderately contaminated	80≤ERI＜160	Considerable risk		
$3<P_{Ag}\leq5$	Moderately polluted	$2<P_{N\text{-}Ag}\leq3$	Moderately polluted	$2<I_{geo}\leq3$	Moderately to heavily contaminated	160≤ERI＜320	High risk		
$P_{Ag}>5$	Heavily polluted	$P_{N\text{-}Ag}>3$	Heavily polluted	$3<I_{geo}\leq4$	Heavily contaminated	ERI≥320	Very high risk		
				$4<I_{geo}\leq5$	Heavily to extremely contaminated				
				$I_{geo}>5$	Extremely contaminated				

2.4 Data processing

To visualize the spatial heterogeneity of contamination by silver ions, geostatistical modeling was performed using the interpolation algorithm of Inverse Distance Weighting (IDW) within the environment of ArcGIS 10.3 (Esri Inc., Redlands, CA, USA). This method was selected to generate continuous surfaces of spatial distribution from discrete points of sampling, effectively capturing the regional gradients of concentration. All statistical treatments were conducted using SPSS 25.0 (IBM Corp., Armonk, NY, USA). Descriptive

statistics, including the mean, the standard deviation, and the coefficient of variation, were calculated to characterize the central tendency and the dispersion of the dataset. The visualization of data and the generation of graphical representations were completed using Origin 2018 (OriginLab Corp., Northampton, MA, USA).

3.Results and Discussion

3.1 Characteristics of concentration for silver ions

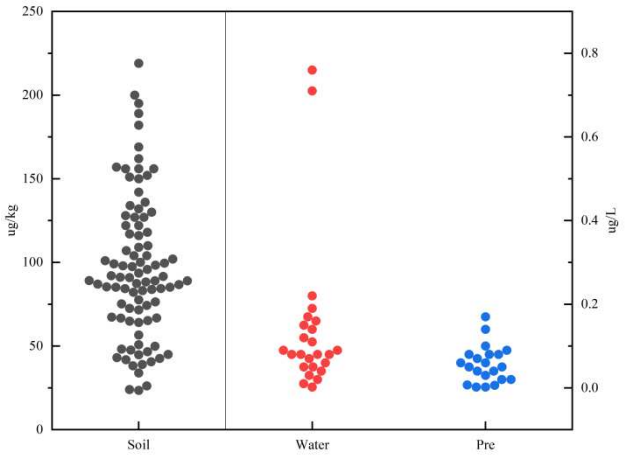


Fig.2. concentration of silver ions in soil, surface water and precipitation

The profiles of concentration for silver ions (Ag^+) across multiple media in the northeastern region of the Tibetan Plateau are statistically summarized in Table 3 and visually clustered in Fig. 2. In the pedological environment, the concentrations of Ag^+ in the soil exhibited a broad range from 23.50 to 272 μg/kg. The regional mean (99.95 μg/kg) and median (91.00 μg/kg)) values align closely with the established value for the background of soil in China (100 μg/kg), indicating the absence of widespread, diffuse contamination across the plateau. However, the maximum recorded value (272 μg/kg) approaches nearly threefold the limit of the background, providing a critical signal for localized enrichment driven by specific inputs from anthropogenic point sources. In stark contrast, matrices in the aqueous phase maintained baseline levels at ultra-trace scales. The concentrations in surface water and precipitation averaged 0.14 μg/L and 0.07 μg/L, respectively. As distinctly illustrated by the clustering of data in Fig. 2, these levels in the aqueous phase remain consistently two orders of magnitude below both the national standards for drinking water in China and the maximum allowable concentration (50 μg/L) established by the WHO. This confirms that the baseline risks to aquatic health associated with the current levels of silver are negligible.

Despite the generally low baselines of concentration, the analysis of the Coefficient of Variation (CV) (Table 3) revealed extreme heterogeneity in space across all media of the environment, descending in the order of surface water (129.21%) > precipitation (57.96%) > soil (48.90%). Such highly elevated values for the CV (>35\%) are robust indicators that the spatial distribution of Ag^+ is heavily governed by localized disturbances of anthropogenic origin rather than the uniform weathering of natural geology. While the accumulation in soil is traditionally linked to legacy sources such as the regional extraction of minerals or localized emissions from industry, the pronounced variability in the hydrosphere and atmosphere indicates the influence of modern inputs of a transient nature. Notably, the atmospheric deposition of Ag^+, captured in precipitation, overlaps with regions subject to the intensive artificial modification of weather. The systematic introduction of catalysts of silver iodide (AgI) into the troposphere to enhance the regional resources of cloud water acts as a direct, albeit trace-level, pathway for atmospheric input. Nevertheless, because the current concentrations in the aqueous phase remain three orders of magnitude lower than the levels in the pedological phase (ng/L vs. μg/kg), the total burden on the environment remains predominantly overshadowed by the historical accumulation in solid phases rather than modern interventions of atmospheric cloud-seeding.

Table 3

Statistical summary of silver ions concentrations of samples(n = 251, ug kg^{-1} for soil and ug L^{-1} for surface water and precipitation).

Sample type	Maximum	Minimum	Mean	Median	STD	coefficient of variation	background value/thresholds
Soil	272	23.50	99.95	91.00	48.87	48.90%	100*
Surface water	0.76	0.01	0.14	0.08	0.19	129.21%	50**
Precipitation	0.17	0.02	0.07	0.06	0.04	57.96%	50**

*Background values for soils in the Chinese region(Wei et al., 1991)

**Chinese National Standard for drinking water(GB 5749-2022), Chinese National Standard for Groundwater(GB/T 14848-2017) and World Health Organization

To further contextualize the integrity of the environment on the plateau, the sub-basins of the region were benchmarked against data at national and global scales (Table 4). Within Qinghai Province, a subtle gradient of spatial distribution is evident: the Qilian Mountains and the Qaidam Basin exhibited relatively higher average concentrations in the soil (107.71

μg/kg and 99.07 μg/kg, respectively) than the pristine region of the Three-River Source (94.03 μg/kg), reflecting mineralogy at localized scales and the footprints of proximal industry. Crucially, however, all sub-regions maintained levels of Ag^+ in the soil that were consistently below the averages reported in heavily industrialized provinces of China (e.g., Beijing: 590 μg/kg; Hunan: 550 μg/kg) and at least an order of magnitude lower than the sinks of sewage sludge reported at a global scale. This stark contrast highlights the absence of accumulation of silver driven by urban wastewater on the plateau. Similarly, the concentrations in surface water across the area of study remained exceptionally low, particularly in the Qilian Mountains (0.07 μg/L). This robust matrix of comparison solidifies the conclusion that the environment across multiple spheres in the northeastern region of the Tibetan Plateau retains a high degree of ecological purity relative to urbanized and industrialized centers at a global scale.

Table 4

Silver ions concentrations in soil, surface water and precipitation from different region(ug kg^{-1} for soil and ug L^{-1} for surface water and precipitation).

Region	Soil	Surface water	Precipitation	Reference
Qilian Mountains	107.71	0.07	0.09	This study
Three River Source	94.03	0.16	0.05	This study
Qaidam Basin	99.07	0.16	0.05	This study
Qinghai	99.95	0.14	0.07	This study
China	100[a]130[b]	/	/	[a](Wei et al., 1991);[b](Xing and Zhu, 2003)
Beijing	590	/	/	(Yao et al., 2010)
Hunan	550	/	/	(Yao et al., 2010)
Sichuang	197	/	/	(Xing and Zhu, 2003)
Fujian	120	/	/	(Chen and Chen, 1992)
Yarlung Tsangpo River	90		/	(Li et al., 2020)
Japan	190-290	/	/	(Hou et al., 2006)
Sewage sludge in China	2720	/	/	(Chen et al., 2020)
Sewage sludge in Czech	1300	/	/	(Urbanová et al., 2013)
Sewage sludge in Sweden	7400	/	/	(Eriksson, 2001)
Chemical factory in China	1220	/	/	(Chen et al., 2022)

3.2 Spatial distribution of silver ions

The patterns of spatial distribution for silver ions (Ag^+) across different media of the environment (Fig. 3) provide critical insights into both the natural connectivity of hydrology

and localized disturbances of anthropogenic origin. The spatial variation of Ag^+ in the soil reveals a pronounced geochemical gradient from east to west, characterized by significant enrichment in the eastern sector relative to the pristine hinterlands of the west. Two primary hotspots of accumulation were identified: the central region of the Qilian Mountains (encompassing Datong and Huzhu Counties) and the central zone of the Three-River Source region (centered on Maqin and Guinan Counties). In these relatively populated and industrialized zones, the concentrations of Ag^+ in the soil approached 300 μg/kg, providing clear spatial signals of contamination from point sources. Conversely, extensive areas of minimal accumulation (< 60 μg/kg) were observed in the arid Qaidam Basin to the west and the southern tier of the Three-River Source region (Fig. 3a). Statistically, 58% of all sampled sites remained below the national value for the background of soil in China (100 μg/kg), confirming that despite localized hotspots in the east, the vast majority of Qinghai Province retains an unpolluted baseline. Mirroring the pedological profile, the distribution of Ag^+ in surface water exhibited a highly consistent gradient from east to west, indicating a strong geochemical coupling between the land and the water. Hotspots of aqueous accumulation were similarly concentrated within the eastern sector of the Three-River Source region (the prefectures of Hainan and Huangnan). However, despite these localized elevations, absolute concentrations remained well within the regulatory limits for safety. Throughout the western zone of the Three-River Source region, the Qilian Mountains, and the Qaidam Basin, the levels in surface water were distinctly suppressed (Fig. 3b). Overall, 88% of all sites of sampling recorded concentrations of Ag^+ below 0.2 μg/L, demonstrating the pristine nature of the hydrosphere in the region and suggesting that terrestrial runoff is the primary, albeit trace-level, driver of silver in the aqueous phase.

In stark contrast to the terrestrial and hydrological matrices, the spatial distribution of Ag^+ in precipitation presented an inverse pattern. Elevated deposition from the atmosphere was primarily concentrated in the territories of the west and the north, specifically the arid Qaidam Basin, the western zone of the Three-River Source region, and the Qilian Mountains (Fig. 3c). While 90% of all samples of precipitation maintained levels at ultra-trace scales (< 0.1 μg/L), this distinct enrichment in the west and the north directly overlaps with strategic zones for the long-term artificial modification of weather. The elevated loading of Ag^+ in

rainfall across these specific catchments strongly suggests the localized "scavenging effect" of catalysts of silver iodide (AgI) for cloud-seeding in the atmosphere, effectively decoupling the footprint of silver in the atmosphere from the industrial emissions based on the ground that are concentrated in the east.

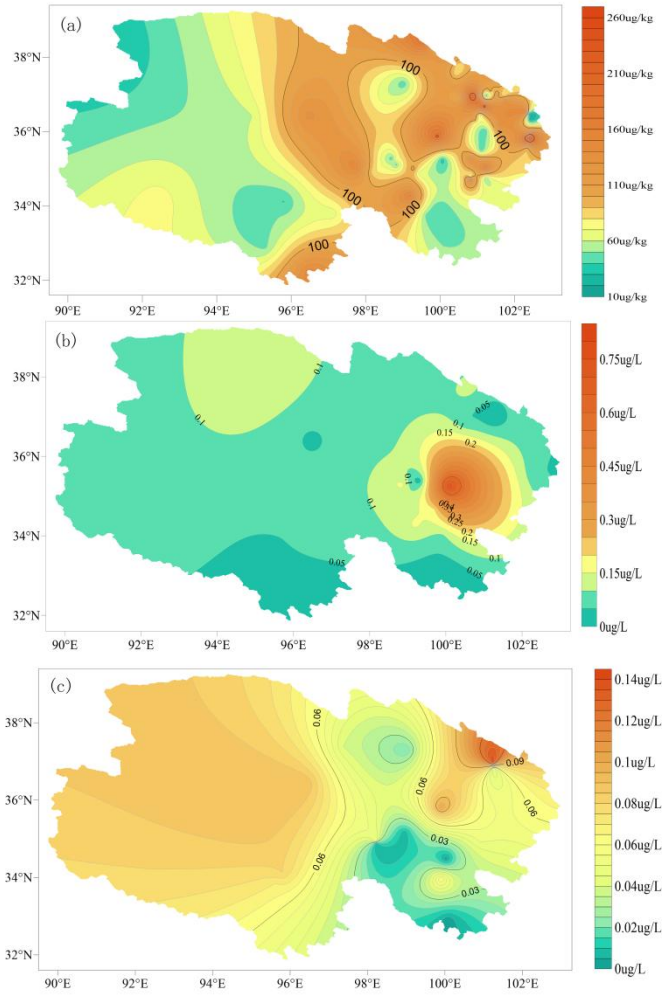


Fig.3. Spatial distribution of silver ions in soil(a),surface water(b) and precipitation(c)

3.3 Assessment of pollution by silver ions

To systematically evaluate the degree of contamination and the enrichment of silver of anthropogenic origin, a strategy of assessment using multiple indices—including the Single Factor Pollution Index (P_{Ag}), the Nemerow Pollution Index ($P_{N\text{-}Ag}$), and the Geo-accumulation Index (I_{geo})—was applied strictly to the environment of the soil. As established in Section 3.1, matrices in the aqueous phase (surface water and precipitation) currently maintain pristine concentrations at the baseline well below stringent limits of regulation. Therefore, this assessment based on indices focuses exclusively on evaluating the

emerging stress within the matrix of the soil (Fig. 4 and Table 5).

The statistical analysis of the index of a single factor (P_{Ag}) reveals a regional environment of the soil in transition. As detailed in Table 5 and the distributions of statistics in Fig. 4, while the regional median for P_{Ag} in Qinghai Province remained within the unpolluted range (0.911), the mean for the province (1.003) narrowly crosses the threshold into mild pollution at localized scales. Among the sub-regions, the Qilian Mountains and the Qaidam Basin exhibited the highest regional means (1.085 and 1.040, respectively), with the distributions of statistics for these areas showing a distinct upward shift compared to the pristine region of the Three-River Source. Spatially, the map for the distribution of P_{Ag} (Fig. 4, top left) corroborates this heterogeneity: although 61% of the sites of sampling remained unpolluted ($P_{Ag} \leqslant 1$), a substantial 35% have degraded into the category of "mildly polluted" ($1 \leqslant P_{Ag} \leqslant 2$), and a marginal 4% exhibit "moderate pollution" ($2 \leqslant P_{Ag} \leqslant 3$). These emerging signals of pollution are highly clustered in the industrialized sector of the east (e.g., Xining and Haidong) and specific zones within the Qilian Mountains. To account for the disproportionate impact on the environment from these localized hotspots of high concentration, the Nemerow Index ($P_{N\text{-}Ag}$) was evaluated. The values for $P_{N\text{-}Ag}$ across all sub-regions ranged from 1.197 (the Three-River Source) to 1.447 (the Qaidam Basin), classifying the comprehensive regional quality of the soil as "slightly polluted" ($1 \leqslant P_{N\text{-}Ag} \leqslant 2$). The elevation of the Nemerow index above the baseline of the single factor emphasizes how discrete, intense zones of accumulation severely degrade the broader rating for the regional quality of the environment, despite the overall low background of the region.

Table 5

Grading of silver ions pollution in the research region.

Pollution index	Region	Maximum	Minimum	Mean	Median	Assessment
P_{Ag}	Qilian Mountains	2.6	0.235	1.085	0.986	Unpolluted
	Three River Source	2.19	0.339	0.928	0.848	
	Qaidam Basin	2.72	0.24	1.04	0.838	
	Qinghai	2.720	0.235	1.003	0.911	
I_{geo}	Qilian Mountains	0.794	-2.674	-0.603	-0.606	Practically uncontaminated
	Three river source	0.546	-2.146	-0.86	-0.824	
	Qaidam Basin	0.859	-2.644	-0.841	-0.839	
	Qinghai	0.858	-2.674	-0.751	-0.7194	

$P_{N\text{-}Ag}$	Qilian Mountains	1.407	Slightly polluted
	Three River Source	1.197	Slightly polluted
	Qaidam Basin	1.447	Slightly polluted
	Qinghai	1.4309	Slightly polluted

Finally, the analysis of I_{geo} was employed to rigorously isolate the enrichment of anthropogenic origin from the fluctuations of natural lithology. As illustrated in the panels at the bottom of Fig. 4, the regional mean values for I_{geo} across all sub-regions remained below 0, classifying the broader plateau as practically uncontaminated relative to baselines from the pre-industrial era. However, the plots of the violin type (Fig. 4, bottom right) reveal a critical extension at the upper tail, particularly in the Qilian Mountains and the overall data for the province. Approximately 16% of individual sites for the sampling of soil have transitioned into the class of "uncontaminated to moderately contaminated" ($0 \leqslant I_{geo} \leqslant 1$). This critical finding confirms that the observed accumulation of silver in the hotspots of the east and the north has unequivocally transcended the weathering of natural geology. It points directly to continuous inputs of anthropogenic origin—such as legacy emissions from industry and deposition across multiple spheres—as the primary drivers fundamentally shifting the baseline of geochemistry for the northeastern region of the Tibetan Plateau.

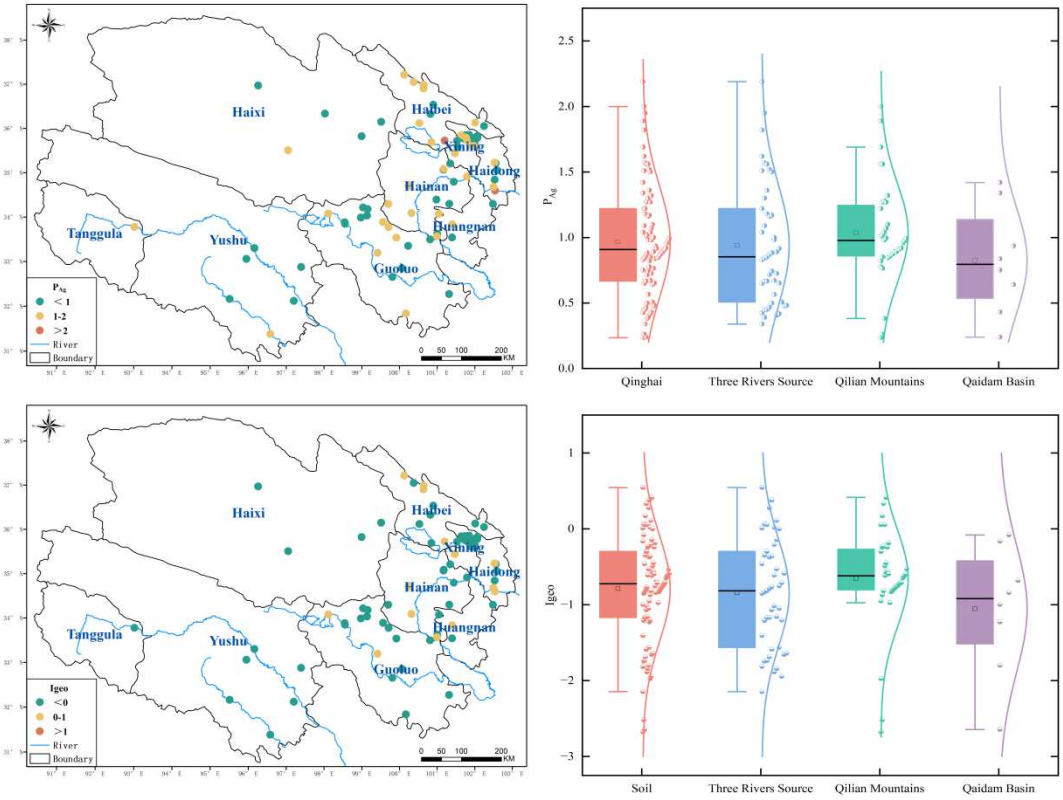


Fig.4. Spatial distribution and statistical variation of pollution indices (P_{Ag} and I_{geo}) exclusively in the topsoil

3.4 Assessment of risk for silver ions

3.4.1 Risk to the ecology

In strict accordance with the framework of the corrected methodology, the Index of Potential Ecological Risk (ERI) was applied exclusively to the environment of the soil (matrix of the soil) to quantify the hazards of a biological nature posed by the accumulation of silver. Because silver possesses an exceptionally high toxicity of a biological nature and sensitivity in the environment (factor of toxic response, T_{Ag}=19), accurately delineating the potential threat to the ecology is imperative, even when the total concentrations of mass appear relatively modest compared to heavy metals from legacy sources. The results of the assessment, summarized spatially and statistically in Fig. 5, reveal a generally controllable yet spatially heterogeneous profile of risk to the ecology. Across Qinghai Province, the values for ERI in the soil exhibited a broad range from 4.47 to 41.61. As illustrated by the plots of the violin type (Fig. 5, right), the vast majority of the sites for the sampling of soil (approximately 99%) fall well below the critical threshold for safety, classifying them as "low risk" (ERI<40). This robust baseline of statistics confirms that, on a scale of the macro-region, silver does not currently pose a widespread or acute threat to the terrestrial ecosystems in the northeastern region of the Tibetan Plateau. However, a closer examination of the distributions of statistics at the sub-regional scale reveals distinct heterogeneity in space. The Qilian Mountains recorded the highest median value for ERI, with the distribution of data for this region showing a clear upward shift, reflecting emerging stress on the ecology driven by proximal activities of anthropogenic origin. In contrast, the arid Qaidam Basin exhibited the lowest profile of risk, with a tighter spread of data and all values remaining safely below the threshold for risk.

Despite the generally safe baseline for the region, the map of spatial distribution (Fig. 5, left) and the extensions at the upper tail of the plots of the violin type highlight critical outliers at localized scales. Approximately 1% of the points for sampling transitioned into the category of "moderate risk" (40≤ERI < 80). Spatially, these nodes of elevated risk (indicated by markers in yellow) are predominantly clustered within the industrialized and populated

corridors of the northeast. The emergence of these hotspots of moderate risk reveals a crucial reality of the environment: the inherently high toxicity of a biological nature for silver significantly amplifies the stress on the ecology from localized emissions of anthropogenic origin. Consequently, these specific catchments in the east warrant prioritized, long-term monitoring for regulation to prevent further degradation of the baseline.

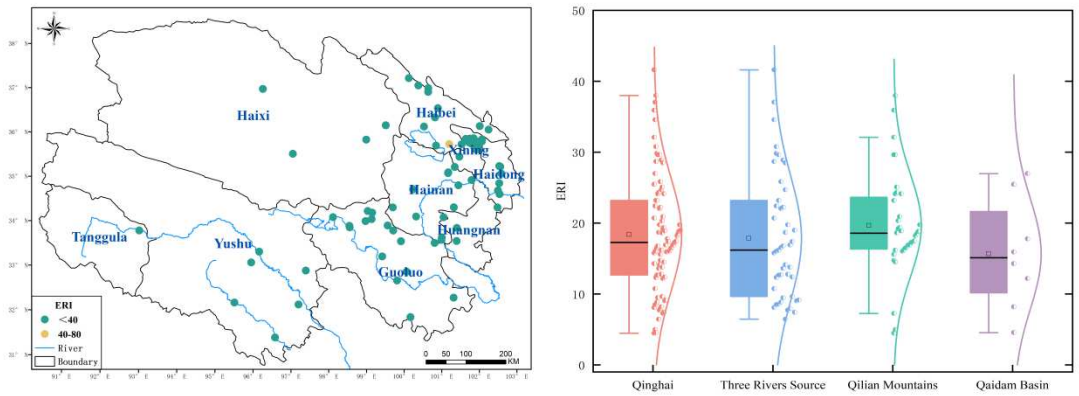


Fig.5. Spatial distribution and regional statistical variation of the Potential Ecological Risk Index (ERI) for silver ions exclusively in topsoils

3.4.2 Assessment of risk to health

To systematically quantify the potential impacts on health of a non-carcinogenic nature from exposure to silver across the environment of multiple spheres, the Hazard Quotient (HQ) was evaluated for both adults and children across varying pathways of exposure. The comprehensive results of the assessment are detailed in Tables 6 and 7, and visually contrasted in Fig. 6. In the environment of the soil, incidental ingestion unequivocally emerged as the primary vector for exposure, contributing orders of magnitude more to the total burden on health than dermal contact and the inhalation of particulates (HQ_{ing}>>HQ_{derm}> HQ_{inh}). Crucially, as evidenced by the updated data in Table 6, all calculated values of HQ for exposure to the soil remained strictly below the critical threshold for safety of 1.0 across all demographic groups and sub-regions. The maximum risk from ingestion (HQ_{ing}) reached only 0.1232 for adults and 0.8805 for children. Although children exhibit a relatively higher susceptibility—driven by lower weights of the body and frequent behaviors from hand to mouth—the chronic risk of a non-carcinogenic nature posed by the accumulation of silver in the soil is universally negligible across the entire northeastern region of the Tibetan Plateau.

For matrices in the aqueous phase, risks to health were evaluated based on the pathway of direct ingestion (Table 7 and Fig. 6b). The direct consumption of surface water poses no threat to health; values for HQ consistently remained well within safe limits, with maximums of 0.3657 for adults and 0.4180 for children. This confirms the robust safety of hydrology for the regional networks of surface water.

Table 6

The hazard quotients(HQ) of silver ions in soil in the research region.

Index	Region	Maximum	Minimum	Mean	Median	Assessment
	Qilian Mountains	0.1125	0.0132	0.0582	0.0550	Negligible
HQ-1	Three River Source	0.1232	0.0191	0.0529	0.0479	Negligible
adult	Qaidam Basin	0.0799	0.0135	0.0464	0.0447	Negligible
	Qinghai	0.1232	0.0132	0.0544	0.0512	Negligible
	Qilian Mountains	0.8041	0.0945	0.4160	0.3930	Negligible
HQ-1	Three River Source	0.8805	0.1363	0.3781	0.3426	Negligible
children	Qaidam Basin	0.5709	0.0965	0.3316	0.3196	Negligible
	Qinghai	0.8805	0.0945	0.3890	0.3655	Negligible
	Qilian Mountains	0.0199	0.0023	0.0103	0.0097	Negligible
HQ-2	Three River Source	0.0218	0.0034	0.0094	0.0085	Negligible
adult	Qaidam Basin	0.0141	0.0024	0.0082	0.0079	Negligible
	Qinghai	0.0218	0.0023	0.0096	0.0091	Negligible
	Qilian Mountains	0.0984	0.0116	0.0509	0.0481	Negligible
HQ-2	Three River Source	0.1078	0.0167	0.0463	0.0419	Negligible
children	Qaidam Basin	0.0699	0.0118	0.0406	0.0391	Negligible
	Qinghai	0.1078	0.0116	0.0476	0.0447	Negligible
	Qilian Mountains	0.0126	0.0015	0.0065	0.0062	Negligible
HQ-3	Three River Source	0.0138	0.0021	0.0059	0.0054	Negligible
adult	Qaidam Basin	0.0089	0.0015	0.0052	0.0050	Negligible
	Qinghai	0.0138	0.0015	0.0061	0.0057	Negligible
HQ-3	Qilian Mountains	0.0233	0.0027	0.0120	0.0114	Negligible

children	Three River Source	0.0255	0.0039	0.0109	0.0099	Negligible
	Qaidam Basin	0.0165	0.0028	0.0096	0.0092	Negligible
	Qinghai	0.0225	0.0027	0.0113	0.0106	Negligible

* HQ-1 is ingestion of HQ; HQ-2 is direct contact of HQ; HQ-3 is inhalation of HQ.

Conversely, the direct ingestion of precipitation without treatment revealed a profile of risk that is anomalous and elevated, breaking the assumption of absolute safety for the region. As depicted in the wide dispersion of data in Fig. 6b, the HQ for precipitation exhibited extreme variability in space, with maximum values surging to 2.1044 for adults and 1.2549 for children. Geographically, this risk of an episodic nature was highly concentrated in the arid Qaidam Basin and the Qilian Mountains. Statistically, 19% of the scenarios of exposure for adults and 9% of those for children significantly exceeded the critical threshold of HQ = 1. This stark contrast between matrices of soil and surface water that are universally safe and precipitation that is episodically hazardous is scientifically revealing. The localized exceedances of the HQ in precipitation are not tied to pollution on the ground from legacy sources, but are intrinsically linked to the "scavenging effect" in the atmosphere. Because the Qilian Mountains serve as strategic zones for the intensive artificial modification of weather, the efficient washout of particulates of silver in the troposphere (e.g., catalysts of silver iodide (AgI) for cloud-seeding) by rainfall of a periodic nature creates transient, concentrated spikes of silver in the aqueous phase. Cumulatively, while the environment of the region is overwhelmingly safe, prioritized advisories for public health are warranted to caution populations of a rural or nomadic nature against the direct harvesting and consumption without treatment of rainwater in these specific hotspots of risk for precipitation.

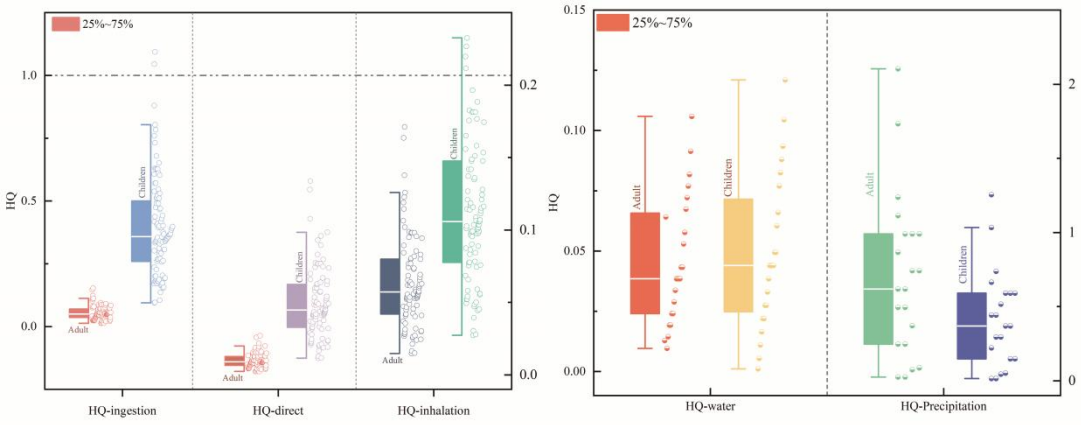


Fig.6. Variation of HQ values through different exposure pathways of silver ions in soil(a), surface water and precipitation samples(b).

The findings across multiple spheres from this study offer critical implications of a dual-sided nature for programs for the regional modification of weather. On a scale of macro-ecology, the universally low values for the Hazard Quotient (HQ < 1) in the topsoil and surface water confirm that operations of cloud-seeding using silver iodide (AgI) spanning decades have not compromised the fundamental integrity of the environment for the "Asian Water Tower". This provides crucial validation of a scientific nature for the continuation of necessary interventions in meteorology aimed at the ecological replenishment of water. However, the detection of episodic, elevated risks to health (HQ > 1) in localized events of precipitation necessitates a shift of the paradigm in operational management. It is recommended that agencies for regional meteorology and the protection of the environment establish coupled networks for monitoring in zones of highly active cloud-seeding (such as the Qilian Mountains). Furthermore, precautionary protocols for public health must be implemented, including the issuance of timely advisories to populations of a rural and nomadic nature to strictly avoid the harvesting and direct consumption of rainwater from the "first-flush" immediately following intensive operations for the artificial enhancement of precipitation.

Table 7

The hazard quotients(HQ) of silver ions in surface water and precipitation in the research region.

Sample type	Index	Region	Maximum	Minimum	Mean	Median	Assessment
Surface water	HQ adult	Qilian Mountains	0.0674	0.0192	0.0375	0.0337	Negligible
		Three River Source	0.1059	0.0096	0.0506	0.0433	Negligible
		Qaidam Basin	0.0722	0.0192	0.0412	0.0385	Negligible
		Qinghai	0.3657	0.0096	0.0694	0.0409	Negligible
	HQ children	Qilian Mountains	0.0770	0.0220	0.0429	0.0385	Negligible
		Three River Source	0.1210	0.0011	0.0566	0.0.0495	Negligible

		Qaidam Basin	0.0825	0.0220	0.0471	0.0440	Negligible
		Qinghai	0.4180	0.0011	0.0762	0.0440	Negligible
		Qilian Mountains	1.7331	0.2476	0.8253	0.4952	Negligible
	HQ	Three River Source	1.2379	0.0248	0.5114	0.6190	Negligible
	adult	Qaidam Basin	2.1044	0.2476	0.9903	0.9903	Negligible
Precipitati		Qinghai	2.1044	0.0248	0.7056	0.6190	Negligible
on		Qilian Mountains	1.0334	0.1476	0.4921	0.2953	Negligible
	HQ-1	Three River Source	0.7382	0.0148	0.3049	0.3691	Negligible
	children	Qaidam Basin	1.2549	0.1476	0.5905	0.5905	Negligible
		Qinghai	1.2549	0.0148	0.4208	0.3691	Negligible

4. Conclusions

This study establishes the first comprehensive baseline across multiple spheres for silver ions (Ag^+)—a critical emerging contaminant of technological origin and an exclusive tracer for the modification of weather—across the northeastern region of the Tibetan Plateau. By integrating sampling across multiple media with rigorous models of risk for geochemistry and the health of humans, the fundamental fate in the environment and the impacts on the ecology from modern interventions of anthropogenic origin in this alpine region were systematically decoded. The principal findings and implications are drawn as follows:

(1) The environment across multiple spheres for the plateau of the region generally maintains a high degree of ecological purity. The concentrations of Ag^+ in the soil closely align with national backgrounds from the pre-industrial era, while surface water and precipitation remain consistently two orders of magnitude below stringent thresholds for safety established by the WHO. However, the indices for pedological evaluation ($P_{N\text{-}Ag}$ and I_{geo}) indicate that the baseline of the region is visibly shifting, transitioning into a state characterized as "slightly polluted" driven by localized enrichment of anthropogenic origin rather than the weathering of natural lithology.

(2) A distinct decoupling in space exists between the distribution of silver across terrestrial and atmospheric matrices. The soil and surface water exhibit a pronounced gradient from east to west, with hotspots of accumulation clustered in the catchments of the east that are populated and industrialized, directly reflecting emissions based on the ground from

manufacturing for emerging high technology and green energy. Conversely, deposition from the atmosphere (precipitation) presents an inverse pattern in space, peaking in the arid Qaidam Basin in the west and the Qilian Mountains. This anomaly in the atmosphere uniquely traces the "scavenging effect" of catalysts of silver iodide (AgI), extensively utilized in regional operations for the artificial seeding of clouds.

(3) While widespread, diffuse risks are absent, the inherently high toxicity of a biological nature for silver (T_{Ag}=19) amplifies localized stress on the ecology, resulting in approximately 1% of the sites for the sampling of soil in the east transitioning into the category of moderate risk to the ecology (ERI$\geqslant$40). From the perspective of the health of humans, chronic risks of a non-carcinogenic nature via contact with the soil and the consumption of surface water are universally negligible (HQ<1) across all demographics. Crucially, however, risks to health of an episodic nature emerged exclusively through the direct ingestion of precipitation without treatment, where up to 19% of the scenarios of exposure for adults in zones for active cloud-seeding exceeded the thresholds for safety.

(4) Ultimately, while the "Asian Water Tower" remains fundamentally secure from widespread contamination by silver, the footprints of the modern expansion of industry and intentional interventions of a meteorological nature are unequivocally detectable. Frameworks for regulation in the future should prioritize targeted controls on emissions in the industrial corridors of the east to prevent further degradation of the baseline for the soil. Furthermore, precautionary advisories for public health are strongly warranted to caution populations of a rural and nomadic nature against the direct harvesting and consumption of rainwater without treatment in the specific sub-regions of the west with high risk.

Declarations:

-Ethics approval and consent to participate:Ethical approval was not required for this study as it did not involve human participants, animals, or human biological materials.

-Consent for publication:Not applicable

-Availability of data and material:The data that support the findings of this study are available from the corresponding author upon reasonable request.

-Competing interests:The authors have no relevant financial or non-financial interests to

disclose.

-Funding:This study is jointly sponsored by the Applied Basic Research Programs of Science and Technology Commission Foundation of Qinghai Province(Grant No. 2026-ZJ-752) and Innovation and Development Special Project of China Meteorological Administration (Grant No.CXFZ2025J043).

-Authors' contributions:Han Huibang: Writing –review & editing, Writing – original draft, Software, Data curation. Zhang Yuxin:Writing – review & editing; Supervision; Project administration. Zhang Liyan:Data curation, Writing – review & editing, Project administration. Guo Shiyu:Data curation, Formal analysis, Investigation, Software. Han Chuntan:Methodology, Validation, Conceptualization, Investigation.

Chen Rensheng:Supervision. Hou Yonghui:Data curation,Validation. Zhang boyue:Data curation,Validation.

-Acknowledgements:The authors gratefully thank the reviewers for their precise and constructive remarks, which significantly helped improve the manuscript.

References

Ahamed, M., AlSalhi, M.S., Siddiqui, M.K.J., 2010. Silver nanoparticle applications and human health. Clinica Chimica Acta. **411**, 1841-1848. https://doi.org/https://doi.org/10.1016/j.cca.2010.08.016.

Bruintjes, R.T., 1999. A Review of Cloud Seeding Experiments to Enhance Precipitation and Some New Prospects. Bulletin of the American Meteorological Society. **80**, 805-820. https://doi.org/https://doi.org/10.1175/1520-0477(1999)080<0805:AROCSE>2.0.CO;2.

Chang, H., Cao, G., Chen, K., Sun, X., 2017. Pollution and Potential Ecological Risk of Heavy Metals in Sediment from the Lower Reaches of Shaliuhe River, Qinghai Lake Watershed. GEOGRAPHICAL SCIENCE. **37**, 259-265. https://doi.org/https://doi.org/10.13249/j.cnki.sgs.2017.02.012.

Chen, B., Xiao, H., 2010. Silver iodide seeding impact on the microphysics and dynamics of convective clouds in the high plains. Atmospheric Research. **96**, 186-207. https://doi.org/https://doi.org/10.1016/j.atmosres.2009.04.001.

Chen, D., Xu, B., Yao, T., Guo , Z., Cui, P., Chen, F., Zhang, R., Zhang, X., Zhang, Y., Fan, J., Hou, Z., Zhang, T., 2015. Assessment of past, present and future environmental changes on the Tibetan Plateau. Chinese Science Bulletin. **60**, 3025-3035. https://doi.org/https://doi.org/10.1360/N972014-01370.

Chen, J., Wang, J., Su, S., 2022. Pollution Characteristics and Evaluation of Silver and Cyanide in Soil of the Relocated Chemical Plant Site. Journal of Shaoyang University(Natural Science Edition). 019. https://doi.org/https://doi.org/10.3969/j.issn.1672-7010.2022.03.012.

Chen, Y., Mao, Y., Song, M., Yin, Y., Liu, G., Cai, Y., 2020. Occurrence and leaching of silver in municipal sewage sludge in China. Ecotoxicology and Environmental Safety. **189**, 109929. https://doi.org/https://doi.org/10.1016/j.ecoenv.2019.109929.

Chen, Z., Chen, C., 1992. Background Values and Characteristics of Soil Elements in Fujian Province. Environmental Monitoring in China. **8**, 4. https://doi.org/https://doi.org/10.19316/j.issn.1002-6002.1992.03.032.

Choi, O., Deng, K.K., Kim, N.-J., Ross, L., Surampalli, R.Y., Hu, Z., 2008. The inhibitory effects of silver nanoparticles, silver ions, and silver chloride colloids on microbial growth. Water Research. **42**, 3066-3074. https://doi.org/https://doi.org/10.1016/j.watres.2008.02.021.

Edition, F., 2011. Guidelines for drinking-water quality. WHO chronicle. **38**, 104-108.

Eriksson, J., 2001. Concentrations of 61 trace elements in sewage sludge, farmyard manure, mineral fertiliser, precipitation and in oil and crops. Swedish EPA - Swedish Environmental Protection Agency (Naturvårdsverket).

Fisher, J.M., Lytle, M.L., Kunkel, M.L., Blestrud, D.R., Dawson, N.W., Parkinson, S.K., Edwards, R., Benner, S.G., 2018. Assessment of Ground-Based and Aerial Cloud Seeding Using Trace Chemistry. Advances in Meteorology. **2018**, 7293987. https://doi.org/https://doi.org/10.1155/2018/7293987.

Guan, X., Su, Y., A, N., Tian, C., Ou, C., Jiang, S., Dinki, B.S., Wang, J., Dang, X., 2024. Research Progress on Remediation of Heavy Metal Pollution in Farmland Soils at Home and Abroad - Based on CiteSpace Knowledge Map Analysis. Chinese Journal of Soil Science. **55**, 573-583. https://doi.org/https://doi.org/10.19336/j.cnki.trtb.2022102001.

Hakanson, L., 1980. An ecological risk index for aquatic pollution control.a sedimentological approach. Water Research. **14**, 975-1001. https://doi.org/https://doi.org/10.1016/0043-1354(80)90143-8.

Han, H., Zhang, Y., Tian, J., Kang, X., 2023. Raindrop Size Distribution Measurements at High Altitudes in the Northeastern Tibetan Plateau during Summer. Advances in Atmospheric Sciences. **40**, 1244-1256. https://doi.org/https://doi.org/10.1007/s00376-022-2186-z.

He, L., Gao, X., 2016. The Accumulation Characteristics and Potential Ecological Risk Assessment of Heavy Metals in Soil of the Three Rivers Source Region: A Case Study in Yushu County, Qinghai Province. Journal of Agricultural Resources and Environment. 1071-1080. https://doi.org/https://doi.org/10.11654/jaes.2016.06.008.

Hou, H., Takamatsu, T., Koshikawa, M.K., Hosomi, M., 2006. Concentrations of Ag, In, Sn, Sb and Bi, and their chemical fractionation in typical soils in Japan. European Journal of Soil Science. **57**, 214-227. https://doi.org/https://doi.org/10.1111/j.1365-2389.2005.00731.x.

Hu, Y., Chen, z., Zhou, X., Liu, M., ZHou, X., 2022. A New Carbon-based Optical Sensor for Detecting Silver Ion in Environmental Water. Biomass Chemical Engineering. **56**. https://doi.org/https://doi.org/10.3969/j.issn.1673-5854.2022.03.002.

Hua, S., Chen, B., Xue, L., Yue, Z., Liu, W., Yang, J., Nie, H., Zhao, S., 2025. Microphysical Responses to Cloud Seeding: Insights From Observation-Validated Simulations. Geophysical Research Letters. **52**, e2024GL114426. https://doi.org/https://doi.org/10.1029/2024GL114426.

Kumar, M., Seth, A., Singh, A.K., Rajput, M.S., Sikandar, M., 2021. Remediation strategies for heavy metals contaminated ecosystem: A review. Environmental and Sustainability Indicators. **12**, 100155. https://doi.org/https://doi.org/10.1016/j.indic.2021.100155.

Li, L., Wu, J., Lu, J., Min, X., Xu, J., Yang, L., 2018. Distribution, pollution, bioaccumulation, and ecological risks of trace elements in soils of the northeastern Qinghai-Tibet Plateau. Ecotoxicology and Environmental Safety. **166**, 345-353. https://doi.org/https://doi.org/10.1016/j.ecoenv.2018.09.110.

Li, S., Yang, J., su, G., Li, Q., Meng, J., Shi, B., 2024. Analysis of heavy metal pollution characteristics and influencing factors in China's typical agricultural areas based on Catboost algorithm. Environmental Chemistry. **43**, 3377-3387. https://doi.org/https://doi.org/10.7524/j.issn.0254-6108.2023041502.

Li, Z., Liu, J., Chen, H., Li, Q., Yu, C., Huang, X., Guo, H., 2020. Water environment in the Tibetan Plateau: heavy metal distribution analysis of surface sediments in the Yarlung Tsangpo River Basin. Environmental Geochemistry and Health. **42**, 2451-2469. https://doi.org/https://doi.org/10.1007/s10653-019-00409-0.

Lin, L., Discussion on the Estimation of Toxicity Coefficients for Heavy Metals Using Toxicological Safety Assessment Data. *China Environmental Protection Federation Energy Environment Professional Committee. 2009 Advanced Symposium on Heavy Metal Pollution Monitoring, Risk Assessment and Remediation Technologies Proceedings* (2009), pp. 60-63.

Liu, H., Gan, Y., Wang, H., Zhang, W., Li, X., Cai, W., Chen, Z., Li, Min, 2024. Silver pollution characteristics and health risks in sewage sludge in the Yangtze River Delta region. Journal of Environmental Engineering Technology. **14**, 1319-1329. https://doi.org/https://doi.org/10.12153/j.issn.1674-991X.20240027.

Long, X., Liu, W., Chou, R., 2024. Research Progress and Prospects of Human Health Risk Assessment of Heavy Metal Pollution in Farmland Soils of China. Acta Pedologica Sinica. **61**, 1188-1200. https://doi.org/https://doi.org/10.11766/trxb202306130229.

Luo Han, Z.Q.Y.X.X.I.L.C.P.W.Q.Y.U.E.P.S.B., 2023. Progress and prospect of cloud precipitation characteristics and cloud water resources exploitation and utilization technology in the Qilian Mountains. Journal of Glaciology and Geocryology. **45**, 368-381. https://doi.org/https://doi.org/10.7522/j.issn.1000-0240.2023.0028.

Ma, Y., Hu, Z., Wang, B., Ma, W., Chen, X., Han, C., Li, M., Zhong, L., Gu, L., Lai, Y., Liu, L., Xie, Z., Han, Y., Yuan, L., Yao, N., Shi, X., 2021. The Review of the Observation Experiments on Land-Atmosphere Interaction Progress on the Qinghai-Xizang （Tibetan） Plateau. Plateau Meteorology. **40**, 1241-1262. https://doi.org/https://doi.org/10.7522/j.issn.1000-0534.2021.zk006.

Muller, G., 1969. Index of Geoaccumulation in Sediments of the Rhine River. GeoJournal. **2**, 109-118.

Newman, P., Meader, N., Klapwijk, P., Chou, E., Gao, Y., Barot, H., Yau, S., Liang, J., Rey, F., Smith, J., 2024. World silver survey 2024. The Silver Institute, Washington, DC.

Oves, M., Khan, M.S., Zaidi, A., Ahmad, E., 2012. Soil Contamination, Nutritive Value, and Human Health Risk Assessment of Heavy Metals: An Overview, in: Zaidi, A., Wani, P.A., Khan, M.S. (Eds.), *Toxicity of Heavy Metals to Legumes and Bioremediation*, Springer Vienna, Vienna, pp. 1-27. https://doi.org/https://doi.org/10.1007/978-3-7091-0730-0_1.

Panyala, N.R., Peña-Méndez, E.M., Havel, J., 2008. Silver or silver nanoparticles: a hazardous threat to the environment and human health? Journal of Applied Biomedicine. **6**, 117-129. https://doi.org/https://doi.org/10.32725/jab.2008.015.

Qu, Z., Han, Q., Yin, D., 2025. Impact of large-scale photovoltaic development on local meteorological conditions. Geographical Research. **44**, 1811-1825. https://doi.org/https://doi.org/10.11821/dlyj020240858.

Rachwał, M., Kardel, K., Magiera, T., Bens, O., 2017. Application of magnetic susceptibility in assessment of heavy metal contamination of Saxonian soil (Germany) caused by industrial dust deposition. Geoderma. **295**, 10-21. https://doi.org/https://doi.org/10.1016/j.geoderma.2017.02.007.

Ramachandra, T.V., Sudarshan, P.B., Mahesh, M.K., Vinay, S., 2018. Spatial patterns of heavy metal accumulation in sediments and macrophytes of Bellandur wetland, Bangalore. Journal of

683 Environmental Management. **206**, 1204-1210.
684 https://doi.org/https://doi.org/10.1016/j.jenvman.2017.10.014.
685 Ratte, H.T., 1999. Bioaccumulation and toxicity of silver compounds: A review. Environmental Toxicology
686 and Chemistry. **18**, 89-108. https://doi.org/https://doi.org/10.1002/etc.5620180112.
687 Rezvani, E., Rafferty, A., McGuinness, C., Kennedy, J., 2019. Adverse effects of nanosilver on human
688 health and the environment. Acta Biomaterialia. **94**, 145-159.
689 https://doi.org/https://doi.org/10.1016/j.actbio.2019.05.042.
690 Sai, N., Qi, J., Jia, Y., Che, M., Yang, J., Wang, X., Xu, C., 2022. Evaluation of soil heavy metal pollution
691 under different land use patterns in the eastern Qilian Mountains. Acta Prataculturae Sinica. **31**,
692 99-109. https://doi.org/https://doi.org/10.11686/cyxb2021394.
693 Schluesener, J.K., Schluesener, H.J., 2013. Nanosilver: application and novel aspects of toxicology.
694 Archives of Toxicology. **87**, 569-576. https://doi.org/https://doi.org/10.1007/s00204-012-1007-z.
695 Suresh, G., Sutharsan, P., Ramasamy, V., Venkatachalapathy, R., 2012. Assessment of spatial distribution
696 and potential ecological risk of the heavy metals in relation to granulometric contents of Veeranam
697 lake sediments, India. Ecotoxicology and Environmental Safety. **84**, 117-124.
698 https://doi.org/https://doi.org/10.1016/j.ecoenv.2012.06.027.
699 Tang, W., Zhang, Z., Zhang, Z., Wang, Y., Chen, Y., Li, S., 2023. Spatial-temporal changes of ecological
700 environment quality in Qinghai Province from 2000 to 2020. Environmental Science & Technology.
701 **46**, 229-237. https://doi.org/https://doi.org/10.19672/j.cnki.1003-6504.0085.23.338.
702 Urbanová, I., Husáková, L., Šrámková, J., 2013. Direct electrothermal atomic spectrometric determination
703 of Ag in aqua regia extracts of soils, sediments, and sewage sludge with matrix modification.
704 Environmental Monitoring and Assessment. **185**, 3327-3337.
705 https://doi.org/https://doi.org/10.1007/s10661-012-2793-8.
706 Wang, Y., Ma, Y., Shi, P., Zhang, G., 2024. The impact of photovoltaic power plant operation on local
707 ecological environments in arid areas. Arid Zone Research. **41**, 1423-1433.
708 https://doi.org/https://doi.org/10.13866/j.azr.2024.08.16.
709 Wei, F., Chen, J., Yu, Y., Zheng, C., 1991. Research on Soil Environmental Background Values in China.
710 Environmental Science. https://doi.org/https://doi.org/10.13227/j.hjkx.1991.04.005.
711 Wu, J., Lu, J., Li, L., Min, X., Luo, Y., 2018. Pollution, ecological-health risks, and sources of heavy
712 metals in soil of the northeastern Qinghai-Tibet Plateau. Chemosphere. **201**, 234-242.
713 https://doi.org/https://doi.org/10.1016/j.chemosphere.2018.02.122.
714 Xing, G., Zhu, J., 2003. *Chemistry of Trace Elements and Rare Earth Elements in Soils*. Science Press.
715 Xu, X., Ma, Y., Sun, C., Wei, F., 2019. Effect of Energy and Water Circulation over Tibetan Plateau.
716 Bulletin of Chinese Academy of Sciences. **34**, 13.
717 https://doi.org/https://doi.org/10.16418/j.issn.1000-3045.2019.11.012.
718 Yang, H., Xu, Y., Sun, S., Gao, H., Deng, R., 2023. Assessment of silver contamination in food using
719 Tb3+-mediated label-free aptasensor. Modern Food Science and Technology. **39**, 284-289.
720 https://doi.org/https://doi.org/10.13982/j.mfst.1673-9078.2023.6.1597.
721 Yao, N., Hou, H., Wang, L., Zhou, Y., Li, F., 2010. Adsorption behavior and speciation transformation of
722 exogenous Ag+ in two typical soils. Environmental Science. **31**, 7.
723 https://doi.org/https://doi.org/10.13227/j.hjkx.2010.04.009.
724 Yao, T., Thompson, L.G., Mosbrugger, V., Zhang, F., Ma, Y., Luo, T., Xu, B., Yang, X., Joswiak, D.R.,
725 Wang, W., Joswiak, M.E., Devkota, L.P., Tayal, S., Jilani, R., Fayziev, R., 2012. Third Pole

Environment (TPE). Environmental Development. **3**, 52-64. https://doi.org/https://doi.org/10.1016/j.envdev.2012.04.002.

Yawei, F., Ziyong, S.U.N., Jianwei, B.U., Hesheng, C.A.I., 2017. The hydrogeochemical characteristics of the river water in the section from Bayi Glacier to Huargzangsi of the Heihe River, Qilian Mountains. Journal of Glaciology and Geocryology. **39**, 680-687. https://doi.org/https://doi.org/10.7522/j.issn.1000-0240.2017.0077.

Zhang, C., Yao, X.-j., Xiao, J.-s., Zhang, H.-f., Wang, Y., Xue, J., 2023. Characteristics of glacier and lake variations in Qinghai province from 2000 to 2020. Journal of Natural Resources. **38**, 822-838. https://doi.org/https://doi.org/10.31497/zrzyxb.20230317.

Zhang, Y., Ma, X., Han, H., Zhang, P., Liu, N., 2021. Analysis of spatial and temporal distribution characteristics of cloud water resources in Qinghai Province from 2014 to 2018. Arid Zone Research / Ganhanqu Yanjiu. **38**. https://doi.org/https://doi.org/10.13866/j.azr.2021.05.07.

Zhao, C., Qu, K., Song, Y., Xu, C., Ren, J., Qu, X., 2010. A Reusable DNA Single-Walled Carbon-Nanotube-Based Fluorescent Sensor for Highly Sensitive and Selective Detection of Ag+ and Cysteine in Aqueous Solutions. Chemistry – A European Journal. **16**, 8147-8154. https://doi.org/https://doi.org/10.1002/chem.201000306.

Zhao, L., Hu, G., Liu, G., Zou, D., Wang, Y., Xiao, Y., Du, E., Wang, C., Xing, Z., Sun, Z., Zhao, Y., Liu, S., Zhang, Y., Wang, L., Zhou, H., Zhao, J., 2024. Investigation, Monitoring, and Simulation of Permafrost on the Qinghai-Tibet Plateau: A Review. Permafrost and Periglacial Processes. **35**, 412-422. https://doi.org/https://doi.org/10.1002/ppp.2227.

Zhou, H., Zhou, H., Xiao, H., Ma, Y., Li, L., Zhang, D., Chen, J., 2020. The Variation Characteristics of Heavy Metal Content,Nutrient and Enzyme Activity in Soil of Alpine Steppe with Different Degradation Gradient in the Three River-Headwaters Region. Acta Agrestia Sinica. **28**, 784-792. https://doi.org/https://doi.org/10.11733/j.issn.1007-0435.2020.03.024.